Inorganic Chemistry

Article

pubs.acs.org/IC

Synthesis, Spectroscopic Characterization, and Determination of the Solution Association Energy of the Dimer $[Co\{N(SiMe_3)_2\}_2]_2$: Magnetic Studies of Low-Coordinate Co(II) Silylamides $[Co\{N(SiMe_3)_2\}_2L]$ (L = PMe_3, Pyridine, and THF) and Related Species That Reveal Evidence of Very Large Zero-Field Splittings

Aimee M. Bryan,[†] Gary J. Long,*[,‡] Fernande Grandjean,*[,‡] and Philip P. Power*[,†]

[†]Department of Chemistry, University of California, Davis, One Shields Avenue, Davis, California 95616, United States

[‡]Department of Chemistry, Missouri University of Science and Technology, University of Missouri, Rolla, Missouri 65409, United States

Supporting Information

ABSTRACT: The synthesis, magnetic, and spectroscopic characteristics of the synthetically useful dimeric cobalt(II) silylamide complex $[Co\{N(SiMe_3)_2\}_2]_2$ (**1**) and several of its Lewis base complexes have been investigated. Variable-temperature nuclear magnetic resonance (NMR) spectroscopy of **1** showed that it exists in a monomer−dimer equilibrium in benzene solution and has an association energy (ΔG_{reacn}) of −0.30(20) kcal mol^{-1} at 300 K. Magnetic data for the polycrystalline, red-brown $[Co\{N(SiMe_3)_2\}_2]_2$ (**1**) showed that it displays strong antiferromagnetic exchange coupling, expressed as $-2J_{ex}S_1S_2$, between the two $S = {}^3/_2$ cobalt(II) centers with a J_{ex} value of −215(5) cm^{-1}, which is consistent with its bridged dimeric structure in the solid state. The electronic spectrum of **1** in solution is reported for the first time, and it is shown that earlier reports of the melting point, synthesis, electronic spectrum, and magnetic studies of the monomer "$Co\{N(SiMe_3)_2\}_2$" are consistent with those of the bright green-colored tetrahydrofuran (THF) complex $[Co\{N(SiMe_3)_2\}_2(THF)]$ (**4**). Treatment of **1** with various Lewis bases yielded monomeric three-coordinated species—$[Co\{N(SiMe_3)_2\}_2(PMe_3)]$ (**2**), and $[Co\{N(SiMe_3)_2\}_2(THF)]$ (**4**), as well as the previously reported $[Co\{N(SiMe_3)_2\}_2(py)]$ (**3**)—and the four-coordinated species $[Co\{N(SiMe_3)_2\}_2(py)_2]$ (**5**) in good yields. The paramagnetic complexes **2**−**4** were characterized by electronic and ^1H NMR spectroscopy, and by X-ray crystallography in the case of **2** and **4**. Magnetic studies of **2**−**5** and of the known three-coordinated cobalt(II) species $[Na(12\text{-crown-}4)_2][Co\{N(SiMe_3)_2\}_3]$ (**6**) showed that they have considerably larger $\chi_M T$ products and, hence, magnetic moments, than the spin-only values of 1.875 emu K mol^{-1} and 3.87 μ_B, which is indicative of a significant zero-field splitting and *g*-tensor anisotropy resulting from the pseudo-trigonal crystal field. A fit of $\chi_M T$ for **2**−**6** yields a large *g*-tensor anisotropy, large negative *D*-values (between −62 cm^{-1} and −82 cm^{-1}), and *E*-values between ±10 cm^{-1} and ±21 cm^{-1}.

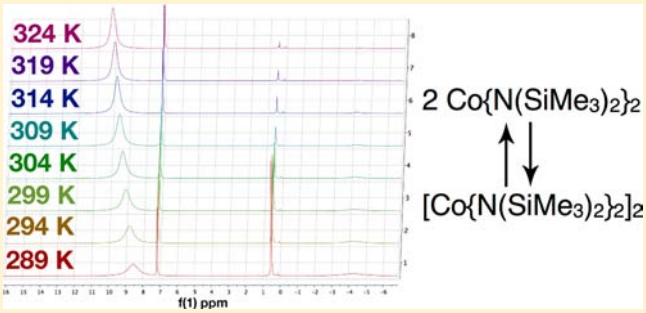

INTRODUCTION

Over 50 years ago, Burger and Wannagat used the silylamido ligand $-N(SiMe_3)_2$ to obtain a series of stable, low-coordinate (coordination numbers of two or three) first-row transition-metal complexes.[1a] The synthesis and (partial) characterization of the divalent M(II) derivatives $[Mn\{N(SiMe_3)_2\}_2]$,[1b] $[Co\{N(SiMe_3)_2\}_2]$,[1a] $[Ni\{N(SiMe_3)_2\}_2]$ (unstable),[1b] and the trivalent M(III) complexes $[Cr\{N(SiMe_3)_2\}_3]$[1b] and $[Fe\{N(SiMe_3)_2\}_3]$[1a] were described. Their solubility in hydrocarbons and high volatility suggested that they existed as unassociated molecules. Later work extended the divalent series to include the iron(II) species $[Fe\{N(SiMe_3)_2\}_2]$.[2] This series has proven to be a very useful group of compounds, because they are widely used as hydrocarbon soluble sources of M^{2+} ions (M = Mn, Fe, Co) as starting materials for many syntheses.[3,4] The trivalent metal series also has been extended to include the M^{3+} derivatives of scandium, titanium, vanadium, manganese, and cobalt (i.e., $M\{N(SiMe_3)_2\}_3$, where M = Sc,[5,6] Ti,[5−7] V,[5−7] Mn,[8] and Co[8]) and they were shown to be three-coordinate[9] monomers either in the gas phase by electron diffraction,[10] or in the solid state by X-ray crystallography[9,11−14] or by spectroscopy.[15−18] The divalent compounds $[M\{N(SiMe_3)_2\}_2]$ (M = Mn, Fe, or Co) were also reported to be monomeric in the gas phase by electron diffraction[3] and in hydrocarbon solution by cryoscopy and spectroscopy;[19,20] however, as solids,

Received: August 5, 2013
Published: October 10, 2013

they have been shown, via X-ray diffraction (XRD), to have dimeric structures in which the metal ions were bridged by amido ligands.[20−22] A feature of the investigations of the divalent $[M\{N(SiMe_3)_2\}_2]_2$ (M = Mn, Fe, or Co) complexes and their derivatives has been that their characterization has not generally included quantitative investigations of their magnetic properties. For example, details of the magnetic behavior of $[Mn\{N(SiMe_3)_2\}_2]_2$ and $[Fe\{N(SiMe_3)_2\}_2]_2$ remain unpublished. An investigation of the magnetism of solid "$Co\{N(SiMe_3)_2\}_2$" in the range of 80−300 K by Fisher and Bradley in 1971 produced a magnetic moment of 4.83 μ_B that is independent of temperature in the range of 80−300 K (cf. 3.87 μ_B for a spin-only moment, $S = {}^3/_2$), and they proposed that the high value of the magnetic moment was due to spin−orbit coupling.[19] However, this interpretation was based on the assumption of a monomeric two-coordinate structure that is at variance with the later X-ray crystallographic data, which showed that "$Co\{N(SiMe_3)_2\}_2$" exists as the dimer $[(Me_3Si)_2NCo\{\mu\text{-}N(SiMe_3)_2\}_2CoN(SiMe_3)_2]$ (**1**), in which two three-coordinate Co^{2+} ions are bridged by two $-N(SiMe_3)_2$ ligands, and are also bonded to a terminal $-N(SiMe_3)_2$ amido group.[22] The burgeoning interest in low-coordinate transition-metal derivatives, especially those of iron and cobalt as potential candidates for single molecule magnets,[4,23−26] has added new urgency to the investigation of their magnetic properties. Because of the low number of ligands, these compounds often display high magnetic moments, due to either an orbital contribution to the moment[21−24] or zero-field splitting and *g*-tensor anisotropy resulting from the uniaxial ligand field.[25−29] The position of the divalent silylamides as key synthons for low-coordinate transition-metal derivatives, as well as the apparently contradictory results of the previous data for "$Co\{N(SiMe_3)_2\}_2$", show that further work was warranted. We now describe our investigations of the magnetic properties of $[Co\{N(SiMe_3)_2\}_2]_2$ (**1**) as well as spectroscopic and magnetic properties of its Lewis base adducts $[Co\{N(SiMe_3)_2\}_2(PMe_3)]$ (**2**), $[Co\{N(SiMe_3)_2\}_2(py)]$ (**3**), and $[Co\{N(SiMe_3)_2\}_2(THF)]$ (**4**), $[Co\{N(SiMe_3)_2\}_2(py)_2]$ (**5**), and $[Na(12\text{-crown-}4)_2][Co\{N(SiMe_3)_2\}_3]$ (**6**).[30] The results indicate that the previous synthesis,[1a] melting point,[1a] electronic spectrum,[19] and magnetic data[19] reported for monomeric "$Co\{N(SiMe_3)_2\}_2$" most probably were for the bright green (giftgrün)[1a] complex $[\{Co\{N(SiMe_3)_2\}_2(THF)]$ (**4**), which is readily produced when the synthesis of "$Co\{N(SiMe_3)_2\}_2$" is conducted in THF solvent.[1a]

EXPERIMENTAL SECTION

All manipulations were performed with the use of modified Schlenk techniques or in a Vacuum Atmospheres drybox under N_2 or argon. Solvents were dried and collected using a Grubbs-type solvent purification system[31] (Glass Contour) and degassed by using the freeze−pump−thaw method. All physical measurements were obtained under strictly anaerobic and anhydrous conditions. IR spectra were recorded as Nujol mulls between CsI plates on a Perkin−Elmer 1430 spectrophotometer. UV−visible spectra were recorded as dilute hexane solutions in 3.5 mL quartz cuvettes using an Olis 17 Modernized Cary 14 UV/vis/NIR spectrophotometer. Melting points were determined on a Meltemp II apparatus using glass capillaries sealed with vacuum grease and are uncorrected. Unless otherwise stated, all materials were obtained from commercial sources and used as received. $[Co\{N(SiMe_3)_2\}_2]_2$ (**1**),[1a] $[Co\{N(SiMe_3)_2\}_2(py)]$ (**2**),[32] $[Co\{N(SiMe_3)_2\}_2(py)_2]$ (**5**),[32] and $[Na(12\text{-crown-}4)_2][Co\{N(SiMe_3)_2\}_3]$ (**6**)[30] were prepared according to literature (**2**, **5**, **6**) or modified procedures (**1**).

$[Co\{N(SiMe_3)_2\}_2]_2$ (1). A diethyl ether suspension of $LiN(SiMe_3)_2$[33,34] was synthesized in situ by adding *n*-BuLi (18 mL, 2.5 M solution in hexanes, 0.044 mol) dropwise to $HN(SiMe_3)_2$ (8.4 mL, 0.040 mol) in diethyl ether (40 mL), cooled in an ice bath. The solution was allowed to come to room temperature and stirring was continued for 12 h. The resulting opaque suspension was added dropwise via cannula to a diethyl ether (40 mL) slurry of $CoCl_2$ (2.86 g, 22.0 mmol) chilled in an ice bath. An immediate color change of the slurry from blue to dark green was observed. When the addition was complete, the suspension was warmed to ca. 35 °C and stirred for 12 h. The ether was removed under reduced pressure and the resulting dark green solids were extracted with hexanes (40 mL), which resulted in a dark green solution with a gray precipitate. The solution was then filtered through a Celite padded filter-stick to afford a clear dark-green solution. The hexanes were removed under reduced pressure to give a dark green oil. The oil was distilled as a dark green vapor at ca. 100 °C (5×10^{-2} Torr) using a short-path distillation apparatus. Upon cooling, the vapor solidified to a brown-dark red solid. The solid was dissolved in hexanes (ca. 30 mL) at 65 °C, which afforded an olive-green solution. Cooling slowly to 0 °C gave **1**, in the form of red-olive dichroic crystals. Yield: 5.70 g (ca. 75%). Melting point (Mp): 89−90 °C.[1] Anal. calcd. for **1**: C, 37.96; H, 9.56; N, 7.38. Found: C, 38.89; H, 10.04; N, 7.17. UV-vis/NIR (hexane, nm [ε, M^{-1} cm^{-1}]: 209 [3000], 223 [11000], 281 [3400], 324 [6500], 604 [140], 668 [200]. IR in Nujol mull (cm^{-1}) with CsI plates: 3140, 2890, 2710, 2650, 1450, 1368, 1357, 1340, 1290, 1250, 1239, 1150, 1070, 1010, 955, 918, 880, 840, 828, 810, 794, 726, 710, 657, 600, 348, 265. μ_B in C_6D_6 solution = 4.7(2) (Evans' method). ^1H NMR (400 MHz, C_6D_6, 295 K): 8.97 (br s, $-SiMe_3$, $[Co\{N(SiMe_3)_2\}_2]$, 0.51 (s, $-SiMe_3$ (terminal), $[Co\{N(SiMe_3)_2\}_2]_2$), −4.22 (br s, $-SiMe_3$ (bridging), $[Co\{N(SiMe_3)_2\}_2]_2$) ppm.

$[Co\{N(SiMe_3)_2\}_2(PMe_3)]$ (2). A diethyl ether solution of trimethylphosphine (PMe_3) (0.36 mL, 3.5 mmol) (30 mL) was added dropwise via cannula at 298 K to a 30 mL hexane solution of $[Co\{N(SiMe_3)_2\}_2]_2$ (**1**) (1.09 g, 1.44 mmol), which produced an immediate color change of the solution from dark olive-green to blue-green. The solution was concentrated under reduced pressure until blue-green solids began to form, at which point the solution was warmed to redissolve the solids. The solution was then placed in a −18 °C freezer overnight which afforded **2** as blue-green crystals. Yield: 1.14 g (ca. 86%). Mp: 97−99 °C. UV-vis/NIR (hexane, nm [ε, M^{-1} cm^{-1}]): 605 [60], 653 [30], 715 [90], 888 [8], 1420 [30]. IR in Nujol mull (cm^{-1}) with CsI plates: 2945, 2910, 2840, 1450, 1368, 1240, 1160, 920, 875, 834, 710, 655, 600, 350. ^1H NMR (400 MHz, C_6D_6, 298 K): 189.34 (br s, PMe_3), −24.65 (br s, $-SiMe_3$) ppm. Anal. Calcd. for **2**: C, 39.53; H, 9.95; N, 6.15. Found: C, 39.78; H, 10.38; N, 6.00.

$[Co\{N(SiMe_3)_2\}_2(py)]$ (3). This compound was prepared according to literature procedures.[32] UV-vis/NIR (hexane, nm [ε, M^{-1} cm^{-1}]): 647 [100], 694 [100], 812 [6], 1461 [20]. ^1H NMR (400 MHz, C_6D_6, 298 K): 342.6 (br, *p*-C_6H_5N), 139.9 (br, *m*/*o*-C_6H_5N), 67.8 (br, *m*/*o*-C_6H_5N), −19.2 (br s, $-SiMe_3$) ppm. Anal. Calcd. for **3**: C, 44.50; H, 9.01; N, 9.16. Found: C, 44.57; H, 9.23; N, 9.04.

$[Co\{N(SiMe_3)_2\}_2(THF)]$ (4). THF (15 mL, ca. 180 mmol) was syringed onto solid $[Co\{N(SiMe_3)_2\}_2]_2$ (**1**) (1.28 g, 1.69 mmol) in a Schlenk flask. After stirring for several minutes, the bright green solution was decanted from a small amount of undissolved solids. The THF solution was concentrated under reduced pressure until green solids began to form. The solution was warmed to redissolve the solids and then stored at room temperature overnight, which afforded a mass of **4** in the form of bright green crystals. Yield: 1.20 g (ca. 78%). Mp: 71−73 °C. UV-vis/NIR (hexane, nm [ε, M^{-1} cm^{-1}]): 593 [6], 680 [90], 1565 [10]. IR in Nujol mull (cm^{-1}) with CsI plates: 2980, 2950, 2910, 2900, 2680, 1450, 1375, 1340, 1250, 1080, 1030, 990, 830, 750, 670, 635, 615, 360. ^1H NMR (400 MHz, C_6D_6, 296 K): 166.9 (br, $-CH_2CH_2O-$ or $-CH_2CH_2O-$), 99.5 (br, $-CH_2CH_2O-$ or $-CH_2CH_2O-$), −17.3 (br s, $-SiMe_3$) ppm. Anal. Calcd. for **4**: C, 42.53; H, 9.82; N, 6.20. Found: C, 42.84; H, 10.35; N, 6.10.

dx.doi.org/10.1021/ic402019w | *Inorg. Chem.* 2013, 52, 12152−12160

X-ray Crystallography. Crystals for XRD studies were removed from the Schlenk tube under a stream of nitrogen and immediately covered with hydrocarbon oil (Paratone-N). A suitable crystal was selected, attached to a glass fiber on a mounting pin, and quickly placed in a low-temperature stream of nitrogen (ca. 90 K for **2**, ca. 150 K for **4**).[35] Data for compound **4** were collected at 150 K due to a phase transition that occurred at ca. 140 K. Data for compounds **2** and **4** were obtained on a APEX-II DUO system, using Mo Kα radiation (λ = 0.71073 Å) in conjunction with a CCD detector. A multiscan absorption correction was applied with the program SADABS.[36,37] The structures were solved by direct methods and refined with the SHELXTL (2013) software package, and the thermal ellipsoid plots were drawn using OLEX2 software.[37,38] Refinement was by full-matrix least-squares procedures with all carbon-bound hydrogen atoms included in calculated positions and treated as riding atoms. A summary of crystallographic and data collection parameters for **2** and **4** is given in Table 1.

Table 1. Selected Crystallographic and Data Collection Parameters for Complexes 2 and 4

	$[Co\{N(SiMe_3)_2\}_2(PMe_3)]$ (**2**)	$[Co\{N(SiMe_3)_2\}_2(THF)]$ (**4**)
formula	$C_{15}H_{45}CoN_2PSi_4$	$C_{16}H_{44}CoN_2OSi_4$
formula weight, Fw	455.79	451.82
color, habit	blue-green, needle	bright green, needle
crystal system	monoclinic	orthorhombic
space group	$P2_1/c$	$Pbcn$
a (Å)	15.1133(19)	13.5395(3)
b (Å)	10.0248(13)	11.1656(3)
c (Å)	17.973(2)	17.7402(4)
α (deg)	90.00	90.00
β (deg)	91.745(2)	90.00
γ (deg)	90.00	90.00
V (Å^3)	2721.8(6)	2681.90(11)
Z	4	4
crystal dimensions (mm)	0.32 × 0.27 × 0.14	0.40 × 0.22 × 0.016
T (K)	90	150
d_{calc} (g/cm^3)	1.112	1.119
abs. coefficient μ (mm^{-1})	0.867	0.825
θ range (deg)	2.27−27.55	2.30−27.48
R(int)	0.0331	0.0322
obs reflections [$I > 2\sigma(I)$]	5772	2601
data/restraints/parameters	6259/0/223	3080/46/156
R_1, observed reflections	0.0360	0.0402

Magnetic Studies. The powdered samples of **1**−**6** used for magnetic measurements were sealed under vacuum in 6-mm outer diameter (OD) and 4-mm inner diameter (ID) quartz tubes with a thin shelf and the sample moment was measured using a Quantum Design MPMSXL7 superconducting quantum interference magnetometer. To prevent crystallite reorientation by the applied field, each sample was anchored with eicosane. For each compound, the sample was zero-field-cooled to 2 K and the moment was measured upon warming to 300 K in an applied field of 0.01 T. In order to ensure thermal equilibrium between the powdered sample sealed under vacuum in the quartz tube and the temperature sensor, the moment was measured at a given sensor temperature until a constant value moment was observed; ca. 14 h were required for the measurements between 2 and 300 K. The measured moments were corrected for the presence of eicosane; no quartz tube correction was necessary because the quartz tube extended equally above and below the sample by ca. 5 cm and its contribution was thus negligible. Diamagnetic corrections of −0.000505, −0.000271, −0.000301, −0.000254, −0.000315, and −0.000610 emu/mol, obtained from tables of Pascal's constants, were applied to the measured molar magnetic susceptibilities of **1**−**6**, respectively.[39] Statistical fitting errors are reported below; the actual errors may be as much as twice as large. The 5 K magnetizations of **1**−**4** were subsequently measured in a 0−7 T applied field. No eicosane or diamagnetic corrections were applied to the 5 K magnetization results.

RESULTS AND DISCUSSION

Synthesis. The dimer $[Co\{N(SiMe_3)_2\}_2]_2$ (**1**) was synthesized by a modified version of that described earlier by Bürger and Wannagat[1a] via the addition of $LiN(SiMe_3)_2$[33,34] to a suspension of $CoCl_2$ in diethyl ether (originally the addition of $NaN(SiMe_3)_2$ to $CoCl_2$ in THF), which afforded a dark olive-green solution. Removal of the solvent followed by extraction with hexanes, filtration, concentration, and distillation of the residue afforded $[Co\{N(SiMe_3)_2\}_2]_2$ as an intensely colored dark green vapor, which solidified to a red-brown solid (Mp 89−90 °C, cf. 73 °C in ref 1a). The same synthesis in THF instead of ether affords the THF complex **4**, in preference to **1**, which can be distilled intact (provided temperatures do not exceed ca. 100 °C), as a green oil, which solidifies to give **4** as bright green crystals that melt in the range of 71−73 °C (described as "$Co\{N(SiMe_3)_2\}_2$" in ref 1a). This behavior is analogous to that of its manganese and iron analogues $[M\{N(SiMe_3)_2\}_2(THF)]$, M = Mn[21,40] and Fe,[20] which can be distilled or sublimed at ≤100 °C without significant dissociation of THF. The THF complex $[Co\{N(SiMe_3)_2\}_2(THF)]$ (**4**) can also be obtained by simply dissolving **1** in THF and isolating crystals of the product by concentrating the solution. Complexes **2** and **5** were made by adding the Lewis bases in slight excess to **1** with stirring for several hours. The monopyridine complex **3** was obtained by subliming **5** at ca. 100 °C under reduced pressure (ca. 5−7 mTorr).[32] Complex **6** was synthesized as described earlier.[30] Recrystallization of **1**−**3**, **5**, and **6** at low temperature from hexane produced good yields of the pure products. The PMe_3 complex (**2**) resembles the PPh_3 complex $[Co\{N(SiMe_3)_2\}_2(PPh_3)]$ of Bradley, Hursthouse, and coworkers,[41] which was synthesized by a different route involving the reaction of 2 equiv $LiN(SiMe_3)_2$ with $CoCl_2(PPh_3)_2$.

Structures. The previously published structure of **1** showed that it featured two three-coordinated cobalt(II) ions bridged by two amido ligands and each terminally bonded to one amido ligand.[22] The Co···Co separation was 2.583(1) Å and the terminal and bridging Co−N distances were 1.922(5) and 2.062(4) Å, respectively, with a planar Co_2N_2 core structure as well as trigonal planar coordination at each Co^{2+} ion.[22] A new crystal structure (see Supporting Information) afforded Co···Co = 2.5865(5) Å, a terminal Co−N = 1.9135(12) Å, and an identical Co−N bridging bond length. The Lewis base complex **2** features trigonal planar geometry at Co (Σ^0 = 359.98(7)) with somewhat different P−Co−N angles of 108.03(6)° and 113.80(6)°. The Co−N distances are equal at 1.9159(18) and 1.9160(18) Å. The Co−P distance is 2.3976(7) Å. The crystal structure of **4** shows that it possesses a 2-fold axis of symmetry along the Co−O bond. It features a Co−N distance of 1.9000(15) Å and a Co−O distance of 2.0358(19) Å, with a N−Co−N angle of 141.89(9)°. Its structure resembles that of its iron analogue, $[Fe\{N(SiMe_3)_2\}_2(THF)]$,[20] which has Fe−N and Fe−O distances of 1.916(5) and 2.071(6) Å, respectively (these bond distances are longer than those in **4**, because of the

dx.doi.org/10.1021/ic402019w | Inorg. Chem. 2013, 52, 12152−12160

larger size of the Fe^{2+} ion).[42] Oddly, the N−Co−N angle in **4**, 141.89(9)°, is ca. 2° narrower than that of its iron congener (N−Fe−N = 144.0(3)°), despite the smaller size of cobalt. The Co−N distances in **2** are longer than those in **4**, possibly because of the strong σ-donor characteristics of PMe_3, which increase the electron density at the Co ion and reduces the attraction of the metal for the electronegative $-N(SiMe_3)_2$ ligand. However, the Co−P bond length in **2** is shorter than that of the complex $[Co\{N(SiMe_3)_2\}_2(PPh_3)]$.[41] This may be partly a result of the greater steric crowding in the latter species. The structures of **2** and **4** are illustrated in Figures 1 and 2,

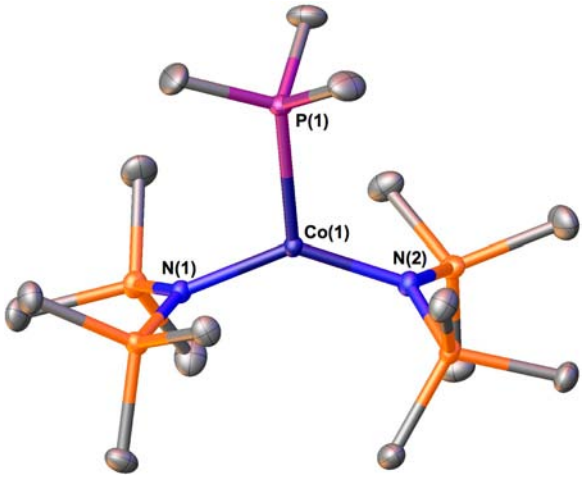

Figure 1. Thermal ellipsoid (50%) drawing of $[Co\{N(SiMe_3)_2\}_2(PMe_3)]$ (**2**). H atoms are not shown for clarity. Selected bond lengths and angles are given in Table 2.

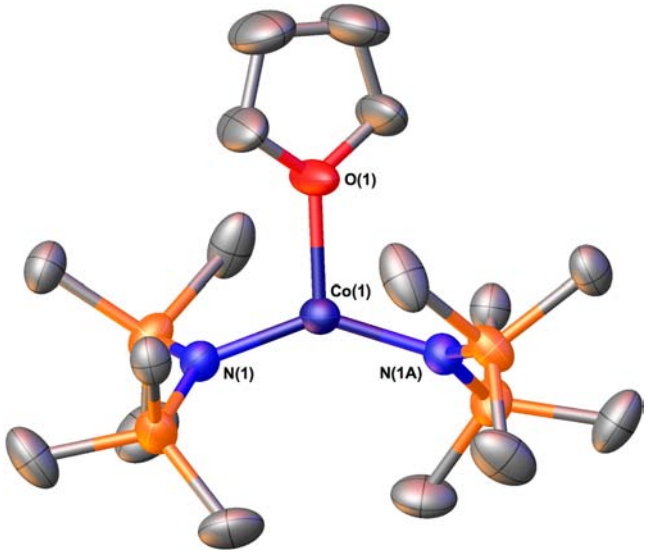

Figure 2. Thermal ellipsoid (50%) drawing of $[Co\{N(SiMe_3)_2\}_2(THF)]$ (**4**). H atoms and disorder are not shown for clarity. Selected bond lengths and angles are given in Table 2.

respectively, and some important bond distances and angles are given in Table 2, along with data for the bispyridine complex **5**, the three-coordinated anion of the ionic complex $[Na(12\text{-crown-}4)_2][Co\{N(SiMe_3)_2\}_3]$ (**6**),[30] and the related species $[Co\{N(SiMe_3)_2\}_2(PPh_3)]$.[41]

It can be seen that the three-coordinated Lewis base complexes (**2**−**4**) all have Co−N distances near 1.9 Å. The previously reported three-coordinated cobalt(II) anion (**6**) has the longest M−N bonds,[30] as a result of interelectronic repulsion produced by the negative charge. Consistent with previous observations,[32] neutral three-coordinated complexes have shorter M−N bonds than those in four coordinate complexes by a margin of 0.06−0.09 Å, except in the case of **6**, which is the most crowded of the compounds, because of the three large $-N(SiMe_3)_2$ ligands and the negative charge, which lengthens the Co−N bonds.

Spectroscopy. The ground state of the free Co^{2+} ion is $^4F_{9/2}$ and the splitting of the free-ion terms for a three-coordinated compound in a D_{3h} ligand field is $^4A_2' + (^4A_1'', {}^4A_2'') + {}^4E'' + {}^4E'$.[17] In idealized D_{3h} symmetry, four $d-d$ transitions are expected. If the symmetry is lowered further, as it is in the three-coordinated Lewis base complexes (**2**−**4**), further splitting of the degenerate ^4E states is expected so that six bands are predicted. The electronic spectrum of **1** in solution was assigned by Fisher and Bradley on the basis of the monomeric formula $Co\{N(SiMe_3)_2\}_2$ and revealed four bands at 409, 585, 685, and 1538 nm with much more intense bands at shorter wavelengths.[19] The electronic spectrum of **1** obtained from a sample synthesized by the method described in the Experimental Section had absorptions at wavelengths of 209, 223, 281, 324, 604, and 668 nm, which are different from those in ref. 19. However, the spectrum of the THF complex **4** in hexane afforded three transitions (nm [ε, M^{-1} cm^{-1}]) observed at at 593 [10], 680 [90], and 1565 [10] over a spectral range of 500−2600 nm, which correspond closely to the three longest wavelength values reported in ref 19. For **2**, in hexane, five transitions (nm [ε, M^{-1} cm^{-1}]) were observed, at 605 [60], 653 [30], 715 [90], 888.8 [8], and 1420 [30]; for **3**, in hexane, four transitions were observed, at 647 [100], 694 [100], 812 [6], and 1461 [20].[32] These absorptions agree with the colors of the series: **1**, red-brown;[1] **2**, blue-green; **4**, bright green; **3**, blue-green;[32] and **5**, aquamarine.[32] Additional absorptions are also observed for **2**−**5** in the shorter-wavelength region (<400 nm).[32] The absorptions below ca. 500 nm in **1** and its complexes have high intensities and are most probably due to ligand-to-metal electron transfer from nitrogen lone pairs to metal d-orbitals. The lower intensities (ε = ca. 10−100 M^{-1} cm^{-1}) of bands in the 500−2600 nm range indicate that they are $d-d$ transitions.

The IR spectra are consistent with previous work.[19,32] The $\nu_{as}(MN_2)$ bands identified in the compounds "$Co\{N(SiMe_3)_2\}_2$" (362 cm^{-1}),[19] $[Na(12\text{-crown-}4)_2][Co\{N(SiMe_3)_2\}_3]$ (368 cm^{-1}),[30] and $[Co\{N(SiMe_3)_2\}_2(py)_2]$ (**5**) (360 cm^{-1})[32] are in agreement with our measurements (**2**, 350 cm^{-1} and **4**, 360 cm^{-1}). The Co−L stretching modes probably appear at lower energies beyond our instrument's lower limit of 250 cm^{-1}, because of their longer and weaker bonds. Other than this basic analysis, full spectral assignments would require full-molecule density functional theory calculations on the series in order to fully interpret the electronic spectra.

NMR Spectroscopy. At ambient temperature, the ^1H NMR spectra of **2**−**4** display large paramagnetic shifts of the Lewis base molecule hydrogens and $-SiMe_3$ signals. Signals due to the latter all appear at upfield shifts in the same spectral region: −24.7 ppm for **2**, −19.2 ppm for **3**, and −17.3 ppm for **4**. The ^1H NMR spectrum for the PMe_3 complex **2** displays one other signal at a chemical shift of 189.3 ppm, which integrates to a 1:4 ratio with respect to the $-SiMe_3$ signal and can thus be readily assigned to the $-PMe_3$ hydrogens. For **3**, based on the

dx.doi.org/10.1021/ic402019w | Inorg. Chem. 2013, 52, 12152−12160

Table 2. Selected Interatomic Distances (Å) and Angles (deg) for Compounds 2−6 and $[Co\{N(SiMe_3)_2\}_2(PPh_3)]$

	$[Co\{N(SiMe_3)_2\}_2(PMe_3)]$ (2)	$[Co\{N(SiMe_3)_2\}_2(py)]$ (3)[a]	$[Co\{N(SiMe_3)_2\}_2(THF)]$ (4)	$[Co\{N(SiMe_3)_2\}_2(py)_2]$ (5)[a]	$[Na(12\text{-crown-}4)_2][Co\{N(SiMe_3)_2\}_3]$ (6)[b]	$[Co\{N(SiMe_3)_2\}_2(PPh_3)]$[c]
			Bond Distances (Å)			
Co−N(1)	1.9159(18)	1.904(3)	1.9000(15)	1.984(1)	1.975(2)	1.931(14)
Co−N(2)	1.9160(18)	1.904(3)		1.983(1)	1.981(2)	1.924(13)
Co−N(3)					1.973(2)	
Co−L	2.3976(7)	2.055(5)	2.0358(19)	2.1135(1) 2.115(1)		2.479(5)
			Bond Angles (deg)			
N(1)−Co−N(1A,2)	138.15(8)	140.7(2)	141.89(9)	123.17(4)	120.50(8), 120.37(8), 119.13(8)	130.7(7)
N(1)−Co−L	108.03(6)	109.7(1)	109.05(4)	90.1(4)		118.5(4)
N(2)−Co−L	113.80(6)	109.7(1)	109.05(4)			110.6(2)
Σ^0 Co	359.98	360.10	359.99		360.00	359.80

[a]Data taken from ref 32. [b]Data taken from ref 30. [c]Data taken from ref 41.

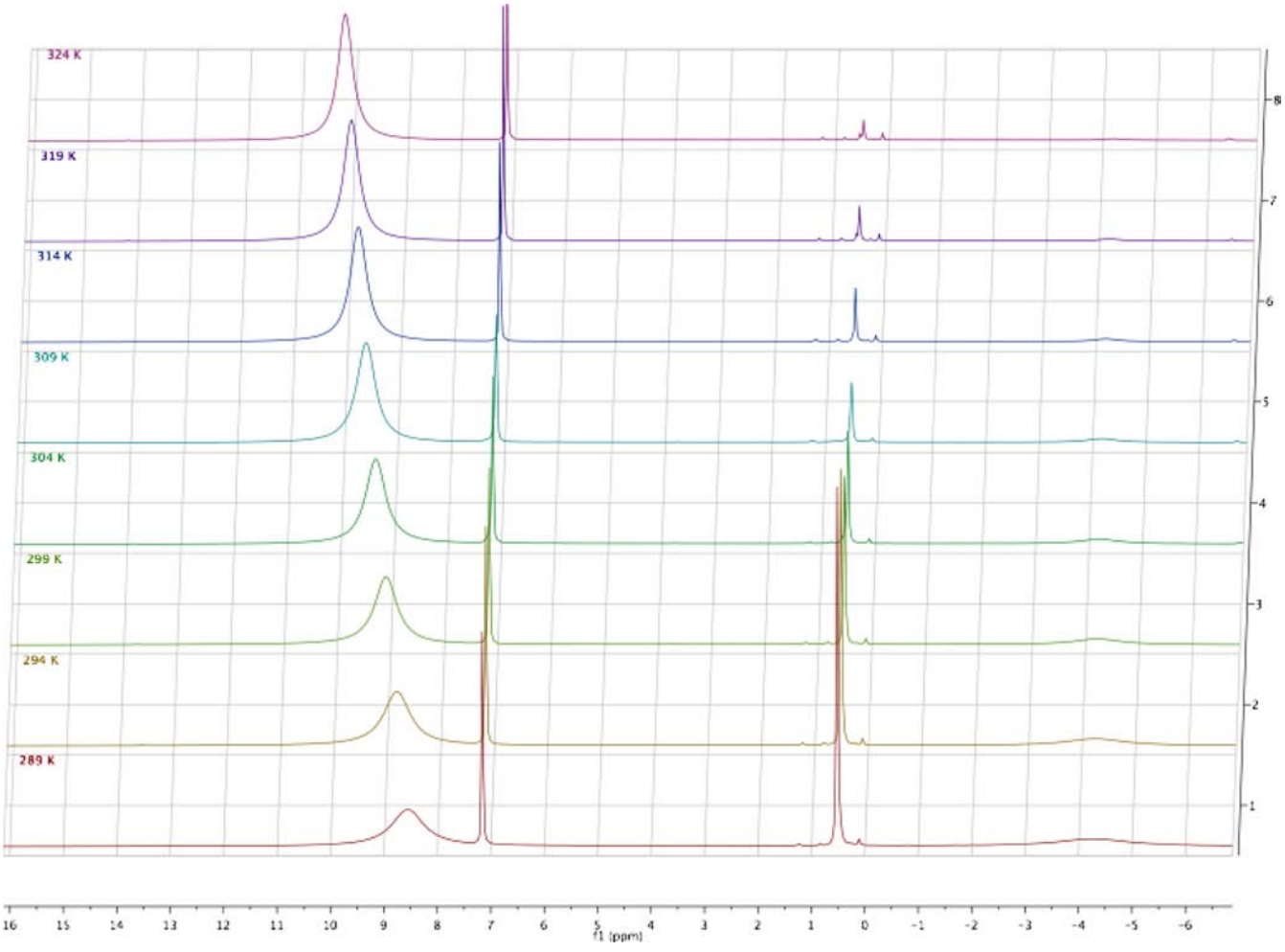

Figure 3. ^{1}H NMR spectra recorded in C_6D_6 for the monomer−dimer equilibrium of **1** in the temperature range 289−324 K.

integrated intensities, the para hydrogen has the furthest downfield shift at 342.6 ppm and the meta and ortho hydrogens are due to absorptions at 139.9 and 67.8 ppm (assignments uncertain). The two methylene $-CH_2-$ resonances of **4** can be assigned to absorptions at 166.9 and 99.5 ppm, based on their equal peak intensities and integration ratios, with respect to the $-N(SiMe_3)_2$ signal.

The variable-temperature ^{1}H NMR (800 MHz, C_6D_6) spectrum of **1** clearly demonstrates evidence of a monomer−dimer equilibrium in solution (Figure 3). An earlier study of the iron(II) analogue $Fe\{N(SiMe_3)_2\}_2$ showed that it was essentially monomeric in solution at room temperature.[20] This is not the case for **1**. At 299 K, the ^{1}H spectrum clearly shows three signals in addition to those of the solvent: a broad signal at 9.09 ppm, which can be assigned to the paramagnetically shifted $-SiMe_3$ protons of the $Co\{N(SiMe_3)_2\}_2$ monomer; a narrower signal at 0.51 ppm; and a broad signal at −4.20 ppm, which can be assigned to the terminal and bridging

dx.doi.org/10.1021/ic402019w | Inorg. Chem. 2013, 52, 12152−12160

$-SiMe_3$ hydrogens of the dimer $[Co\{N(SiMe_3)_2\}_2]_2$. Upon cooling, the dimer signals intensify, with the terminal $-SiMe_3$ signal shifting slightly downfield to 0.52 ppm (289 K) and the bridging $-SiMe_3$ signal shifting upfield to −4.27 ppm (289 K). Simultaneously, the monomer resonance shifts upfield to 8.55 ppm and decreases in intensity. Upon warming to 324 K, the dimer signals essentially disappear and the monomer signal greatly intensifies and is shifted further downfield to 10.18 ppm. The association equilibrium constants for eq 1 using the Van't Hoff equation over the range of 289−324 K and the relative concentrations of monomer and dimer derived from peak integration of a 0.12(1) M solution of the monomer $Co\{N(SiMe_3)_2\}_2$ in C_6D_6 gave values of −20(2) kcal mol^{-1} for ΔH^0_{reacn} and −66(6) cal mol^{-1} K^{-1} for ΔS^0_{reacn}.

$$2Co\{N(SiMe_3)_2\}_2 \rightleftarrows [Co\{N(SiMe_3)_2\}_2]_2 \quad (1)$$

Using these values at 300 K, the ΔG_{reacn} is −0.30(20) kcal mol^{-1}. Compared to the association constants for the iron(II) analogue (−19 kcal mol^{-1} for ΔH^0_{reacn}, −75 cal mol^{-1} K^{-1} for ΔS^0_{reacn} and 3 kcal mol^{-1} for ΔG_{reacn}).[20] The relatively weak association observed for **1** and $[Fe\{N(SiMe_3)_2\}_2]_2$ is supported by the fact that monomeric structures are observed in the crystal phase when one or two of the methyl substituents on each $-SiMe_3$ group are replaced by phenyl groups.[42]

The conclusion from the variable-temperature ^{1}H NMR investigation is that, in concentrations of ca. 0.1 M of $Co\{N(SiMe_3)_2\}_2$ in C_6D_6, the ratio of monomer to dimer is ca. 4:1 at room temperature. Thus, the majority of the sample is monomeric but there is a significant percentage of dimer also present. The free energy of the reaction slightly favors (by ca. −0.30(20) kcal mol^{-1}) the dimeric structure at room temperature in contrast to the corresponding iron(II) amide equilibrium in which the monomer is favored by ca. 3 kcal mol^{-1} at room temperature.[20] Because of the smaller radius of the Co^{2+} ion, and therefore greater steric crowding produced by the $-SiMe_3$ groups, it might be expected that the association energy of the cobalt(II) dimer would be lower than that of the iron analogue, but this is not the case. The stronger association of **1** is supported by the fact that it has a higher melting point than that of its iron congener and because our experience indicates that it distills under reduced pressure at a significantly higher temperature.

Magnetism. It should be remarked that these studies of three- and four-coordinated cobalt(II) complexes are paralleled by magnetic studies on related iron(II) complexes involving $[Fe\{N(SiMe_3)_2\}_2]$ complexed by carbene,[44,45] phosphine,[46] pyridine,[32] and β-diketiminate[47,48] ligands. The magnetic moment for the cobalt(II) amide $Co\{N(SiMe_3)_2\}_2$ (which is assumed to be monomeric, based on the electronic and mass spectroscopy and molecular weight data in cyclohexane solution) was reported to be 4.83 μ_B.[19] This value falls within the range measured for several two-coordinated Co(II) amides (4.1−6.3 μ_B).[4,28,43,49] We investigated the magnetic properties of a polycrystalline sample of $[Co\{N(SiMe_3)_2\}_2]_2$ (shown to have a dimeric structure by X-ray crystallography).[22] The magnetic properties of $[Co\{N(SiMe_3)_2\}_2]_2$ (**1**) have been measured, after zero-field cooling, upon warming from 2 K to 300 K in a 0.01 T applied magnetic field. The results in terms of $\chi_M T$ are shown as the points in Figure 4. The magnitude of $\chi_M T$ is very low, in comparison to that in ref 19, and is indicative of extensive antiferromagnetic exchange between two $3d^7$ cobalt(II) ions with $S = {}^3/_2$ with a second-order Zeeman contribution, $N\alpha$, to the molar magnetic susceptibility. Thus,

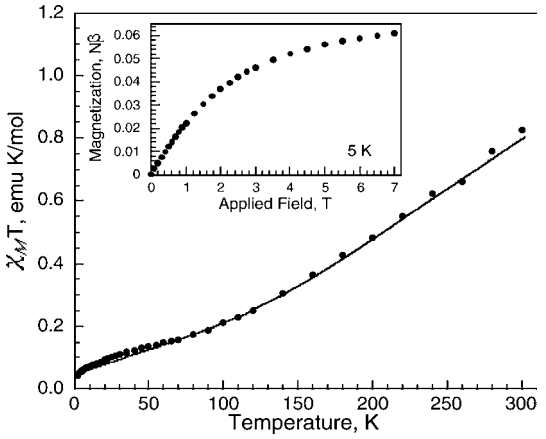

Figure 4. Temperature dependence of $\chi_M T$ obtained at 0.01 T for **1**, black points, and a fit, black line, obtained between 2 and 300 K, for $3d^7$ cobalt(II) and $S_1 = S_2 = {}^3/_2$ and $g = 2$ with $J_{ex} = -215(5)$ cm^{-1}, $N\alpha = 0.00157(5)$ emu/mol, and 2.5 mol % of an impurity of Co(II) with $S = {}^3/_2$ and $g = 2$. Inset shows the magnetization of **1** obtained at 5 K.

the 2−300 K temperature dependence of $\chi_M T$ of **1** has been fit with the Heisenberg isotropic exchange coupling Hamiltonian:

$$H = -2J_{ex}S_1S_2$$

the result of this fit is shown as the line in Figure 4. For $3d^7$ cobalt(II) with $S_1 = S_2 = {}^3/_2$ and $g = 2$, the fit yields $J_{ex} = -215(5)$ cm^{-1}, $N\alpha = 0.00157(5)$ emu/mol, and 2.5 mol % of an impurity of Co(II) (the possibility that this impurity is monomeric $Co\{N(SiMe_3)_2\}_2$ suggests itself, but no evidence for its presence was apparent from the X-ray data) with $S = {}^3/_2$ and $g = 2$. Because of the strong correlation between the parameters, g was not varied but fixed at $g = 2$. Furthermore, there is a correlation between J_{ex} and $N\alpha$, such that probably the best conclusion is that (i) at the lower temperatures, as a result of strong antiferromagnetic exchange, only the $J = 0$ state is populated and (ii) the second-order Zeeman contribution ($N\alpha$) is substantial. These conclusions are fully consistent with the structure of **1** summarized above. The magnetization of **1** has been measured at 5 K and its initial slope agrees well with the 5 K value of χ_M obtained at 0.01 T. As shown in the inset for Figure 4, the 5 K magnetization of **1** is only 0.066 $N\beta$ at 7 T and arises mainly from the 2.5 mol % impurity plus possibly a small contribution from canting of the antiferromagnetically coupled moments. The lower magnetic moment for **1** is consistent with the low magnetic moment (1.72 μ_B), determined for the dimer $[\{Co(NPh_2)_2\}_2]$ via the Evans' method.[50]

We also investigated the magnetism of **1** in C_6D_6 solution via the Evans' method. At a concentration of 0.033 M, a magnetic moment of 4.7(3) μ_B was observed, which is close to the 4.83 μ_B value measured for the putative "$Co\{N(SiMe_3)_2\}_2$" monomer in the solid state.[19] However, this apparent agreement is probably fortuitous. A magnetic moment of 5.883(3) μ_B is reported herein for $[Co\{N(SiMe_3)_2\}_2(THF)]$ (**4**). If the 4.83 μ_B value of ref 19 is corrected for the difference between the molecular weights of the putative monomer "$Co\{N(SiMe_3)_2\}_2$" (mol wt = 379.70 g/mol) and **4** (mol wt = 451.82 g/mol), a value of 5.75 μ_B is obtained, which is consistent with the 5.883(3) μ_B reported herein. The solution magnetic moment of **1**, 4.7(3) μ_B, is consistent with the existence of **1** as dissociated $Co\{N(SiMe_3)_2\}_2$ monomers in solution. The solution magnetic moment is larger than the

dx.doi.org/10.1021/ic402019w | Inorg. Chem. 2013, 52, 12152−12160

expected spin-only magnetic moment of 3.87 μ_B, and is equal to the 4.7 μ_B of the bent geometry two-coordinate species $[Co\{N(H)Ar^{Me_6}\}_2]$ (Ar^{Me_6} = C_6H_3-2,6(C_6H_2-2,4,6-Me_3)$_2$),[28] but is smaller than that of the linearly coordinated species $[Co\{N(H)Ar^{Pr^i_6}\}_2]$ ($Ar^{Pr^i_6}$ = C_6H_3-2,6(C_6H_2-2,4,6-Pr^i_6)$_2$).[28]

The magnetic properties of $[Co\{N(SiMe_3)_2\}_2(L)]$ (**2**–**5**) and $[Na(12\text{-crown-}4)_2][Co\{N(SiMe_3)_2\}_3]$ (**6**) have been measured, after zero-field cooling, upon warming from 2 K to 300 K in an applied magnetic field of 0.01 T; the resulting $\chi_M T$ values are shown as the points in Figure 5. As would be expected for these complexes with no intermolecular exchange, $1/\chi_M$ is almost linear with temperature and Curie–Weiss law fits between 50 and 300 K yield the parameters at the top of Table 3; these are parameters that are indicative of paramagnetic cobalt(II) complexes with $S = {}^3/_2$ in the presence of zero-field splitting. The deviation from Curie–Weiss law behavior below 50 K is indicative of the presence of zero-field splitting of the electronic ground state of the cobalt(II) cations in **2**–**6**. Indeed, very similar magnetic results have been observed for a tetrahedral complex, $\{Co(SPh)_4\}^{2-}$, that exhibits slow magnetic relaxation in a zero applied field.[51] As a result, the $\chi_M T$ observed for **2**–**6** between 2 and 300 K and the 5 K magnetization of **2**–**4** have been simultaneously fit with the PHI code,[52] with a model that assumes the presence of an axial component (D) and a nonaxial component (E) to the zero-field splitting. In these fits, D, E, g_z, and $g_x = g_y$ have been varied and the best fit of $\chi_M T$ and, when available, the 5 K magnetization obtained. The results of the 5 K magnetization calculated for random powder samples are shown in the inset for Figure 5, which shows good agreement for compounds **2** and **3**, but poorer agreement for compound **4**. This poorer agreement for (**4**) may be an indication of some nonrandom orientation of the crystallites in the powder sample used for the magnetic measurements. The resulting fits are shown as the solid lines in Figure 5, and the resulting best fit parameters are given in the lower portion of Table 3. The moments for **5** and **3** were previously reported at 300 K as 4.65 and 4.69 μ_B, respectively. The value for **5** is in excellent agreement with the 4.642(4) μ_B reported in Table 3, but the value for **3** is smaller than the 5.269(3) μ_B reported in Table 3. The earlier measurements may have included larger errors due to smaller sample sizes.[32]

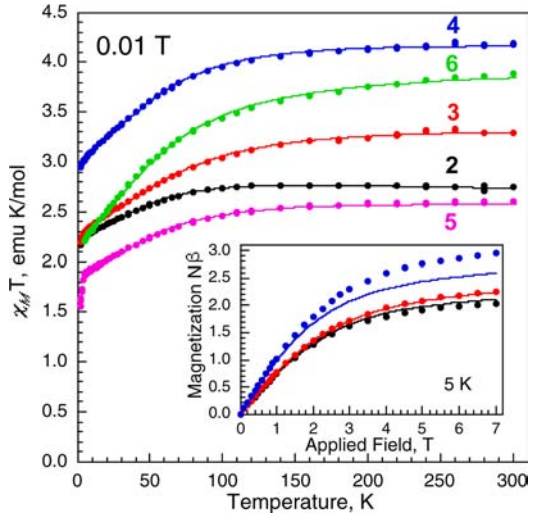

Figure 5. Temperature dependence of $\chi_M T$ obtained at 0.01 T (data points), and the best fits obtained between 2 K and 300 K for **2**–**6** with $S = {}^3/_2$ in the presence of zero-field splitting of the electronic ground state. Inset shows the 5 K magnetization for **2**–**4** and its fit obtained simultaneously with the $\chi_M T$ fit. The resulting best-fit parameters are given in Table 3.

As is well-known, the fit of the temperature dependence of $\chi_M T$ with the zero-field splitting Hamiltonian for $S = {}^3/_2$ is insensitive to the sign of D. The fits reported herein, when D was chosen to be positive, g_z refined to a smaller value than $g_x = g_y$, a g-tensor anisotropy that is not possible[25] for cobalt(II), which has a $3d^7$ electronic configuration and thus a negative spin-orbit coupling parameter.

In view of their similar structures, perhaps the most unexpected magnetic property observed for **2**–**4** is the difference in the magnitude of their $\chi_M T$ values (see Figure 5), differences that are reflected in both the differing D-values and g-values found in Table 3 and reproduced by separate sample preparations. If the ordering of the 3d orbitals in the electrostatic trigonal crystal field, with the z-axis oriented normal to the trigonal plane and passing through the cobalt(II) ion, is $3d_{xz} \approx 3d_{yz} < 3d_{z^2} < 3d_{x^2-y^2} \approx 3d_{xy}$, then the axial zero-field splitting parameter, D, is predicted[53] to be large and positive, in disagreement with the observed negative D-values (see Table 3). In order to achieve a large negative D value through spin–orbit coupling between the electronic ground state and a low-lying excited state, a mixing by spin–orbit coupling[54] must take place between orbitals that have the same m_l value. Such a process is impossible with the above D_{3h} trigonal symmetry d-orbital ordering. However, if the 3d orbital ordering is $3d_{z^2} < 3d_{yz} < 3d_{xz} < 3d_{x^2-y^2} < 3d_{xy}$, as is predicted[47,55] for the approximately C_2 symmetry of compounds **2**–**4**, the mixing by spin–orbit coupling between the $3d^7$ cobalt(II)

Table 3. Magnetic Properties of the $[Co\{N(SiMe_3)_2\}_2(L)]$ Complexes

	$[Co\{N(SiMe_3)_2\}_2(PMe_3)]$ (**2**)	$[Co\{N(SiMe_3)_2\}_2(py)]$ (**3**)	$[Co\{N(SiMe_3)_2\}_2(THF)]$ (**4**)	$[Co\{N(SiMe_3)_2\}_2(py)_2]$ (**5**)	$[Na(12\text{-crown-}4)_2][Co\{N(SiMe_3)_2\}_3]$ (**6**)
			50–300 K, Curie–Weiss Law Fit		
θ, deg	−2.3(4)	−13.8(3)	−9.6(2)	−9.7(2)	−19.8(4)
C, emu K/mol	2.778(6)	3.471(7)	4.328(4)	2.695(5)	4.131(5)
μ_{eff}, μ_B	4.714(5)	5.269(5)	5.883(3)	4.642(4)	5.748(5)
g for $S = {}^3/_2$	2.435(3)	2.722(3)	3.038(1)	2.397(2)	2.968(3)
			2–300 K Fit of $\chi_M T$		
D, cm^{-1}	−74(2)	−82(2)	−73(2)	−66(2)	−62(1)
E, cm^{-1}	±9.6(5)	±21.0(5)	±14.6(5)	±11.0(5)	±10(1)
g_z	2.82(1)	2.84(1)	3.28(1)	2.54(1)	2.75(1)
$g_x = g_y$	2.10(1)	2.57(1)	2.78(1)	2.22(1)	2.97(1)

dx.doi.org/10.1021/ic402019w | Inorg. Chem. 2013, 52, 12152–12160

$3d_{z^2}{}^2 3d_{yz}{}^2 3d_{xz}{}^1 3d_{x^2-y^2}{}^1 3d_{xy}{}^1$ ground-state electronic configuration and the first excited state $3d_{z^2}{}^2 3d_{yz}{}^1 3d_{xz}{}^2 3d_{x^2-y^2}{}^1 3d_{xy}{}^1$ configuration is allowed because the $3d_{yz}$ and $3d_{xz}$ orbitals, orbitals that have the same $m_l = \pm 1$ values, transform with the same B irreducible representation. Then, the mixing of the ground and excited states through the spin−orbit coupling will stabilize[54] the $M_S = \pm^3/_2$ state of the cobalt(II) ion in a compound and lead to a negative D-value. The absolute $|D|$ value is inversely proportional[53] to the energy splitting between the $3d_{yz}$ and $3d_{xz}$ orbitals. Hence, a small (or large) splitting will lead to a large (or small) absolute $|D|$ value. We propose that the differences in D-values observed for compounds **2**−**4** originate in different energy splitting between the $3d_{yz}$ and $3d_{xz}$ orbitals, a splitting that is related to the extent of the structural and electric distortion from ideal C_3 symmetry at the cobalt(II) ion. In compound **3**, where the cobalt(II) ion is bonded to three nitrogens, the splitting is expected to be smaller than in compound **2** or **4**, where the cobalt(II) ion is bonded to two nitrogens and one phosphorus or one oxygen, respectively. Hence, a more negative D-value is expected for compound **3** than for compound **2** or **4**, in agreement with observation.

At this point, it seems that full ab initio studies will be required for a deeper understanding of the mixing by spin−orbit coupling of the various excited states into the electronic ground state to yield the observed differences in $\chi_M T$ and, hence, moments. Furthermore, in view of the interesting magnetic properties of **2**−**6** and their similarity to the dianion $\{Co(SPh)_4\}^{2-}$,[51] AC magnetic susceptibility studies are underway.

CONCLUSIONS

Our detailed study of a representative group of two- and three-coordinated cobalt(II) compounds, which includes two new three-coordinated cobalt(II) silylamides, as well as the synthetically important precursor $[Co\{N(SiMe_3)_2\}_2]_2$ (**1**), provides ample evidence of their interesting magnetic behavior. We have spectroscopically characterized the silylamide $[Co\{N(SiMe_3)_2\}_2]_2$ species for the first time and determined its association energy. The magnetic data for $[Co\{N(SiMe_3)_2\}_2]_2$ (**1**) show that it displays strong antiferromagnetic coupling and the moments for the monomeric three-coordinated species **2**−**4** and **6** are considerably larger than the spin-only $\chi_M T$ product of 1.875 emu K mol^{-1}, and a magnetic moment of 3.87 μ_B. Moreover, these compounds display substantial negative axial zero-field splittings (D) that may be associated with substantial spin reversal barriers.[56] However, the significant rhombicity ($|E/D|$) observed for these compounds may substantially reduce the magnetic anisotropy and the barriers expected, based on the D-values. Although the structural and magnetic data for **1** show that it is a dimer in the solid phase, the solution ^{1}H NMR data show that, in ca. 0.12 M benzene solution, it is extensively dissociated to the monomeric form $Co\{N(SiMe_3)_2\}_2$, which is in agreement with the mass spectral data reported in ref 19. However, a comparison of the electronic spectra of **1** and its THF complex $[Co\{N(SiMe_3)_2\}_2(THF)]$ (**4**) with those reported in ref 19 show that the electronic spectrum given in that paper corresponds closely with those that we have measured for **4**. Moreover, the color of **4** that we observe (bright green) corresponds to that originally reported in ref 1a (giftgrün) for $Co\{N(SiMe_3)_2\}_2$. Thus, it seems that bis(trimethylsilyl)amido cobalt has been misidentified[57] from the beginning.[1a] Further studies are in progress to examine the spin-relaxation barriers of these and other low-coordinate transition-metal compounds, using AC magnetic measurements for the investigation of their potential use as single molecule magnets.

ASSOCIATED CONTENT

Supporting Information

^{1}H NMR spectra of **1**−**4**; Evans' method ^{1}H NMR spectra of **1**; calculations of solution association energy of **1**; CIFs of **1**, **2**, and **4**; IR UV-vis spectra of **1**, **2**, and **4**. Photographs of crystals of **1**−**4**. This material is available free of charge via the Internet at http://pubs.acs.org.

AUTHOR INFORMATION

Corresponding Author

*E-mail addresses: pppower@ucdavis.edu (P.P.P.), glong@mst.edu (G.J.L.).

Notes

The authors declare no competing financial interest.

ACKNOWLEDGMENTS

This research was supported by National Science Foundation (NSF) (through Grant Nos. CHE-1263760 and DBIO 722538). A.M.B. thanks the NSF-Graduate Research Fellowship Program for their financial support (through Grant No. DGE-1148897), Professors M. M. Olmstead and H. Hope for their invaluable crystallographic support, and Professor R. A. Andersen for useful discussion on the magnetism and properties of **1**. We thank a reviewer for drawing our attention to similarities in the electronic spectral data for **4**, also, and those in ref 19, as well as Jerry Dallas and Ping Yu for help with the NMR spectroscopic measurements. Compound **6** and the magnetic data were provided by Chris Melton.

REFERENCES

(1) (a) Bürger, H.; Wannagat, U. *Monatsh. Chem.* **1963**, *94*, 1007−1012. (b) Bürger, H.; Wannagat, U. *Monatsh. Chem.* **1964**, *95*, 1099−1102.
(2) Andersen, R. A.; Faegri, K.; Green, J. C.; Haaland, A.; Lappert, M. F.; Leung, W.-P.; Rypdal, K. *Inorg. Chem.* **1988**, *27*, 1782−1786.
(3) Power, P. P. *Chemtracts* **1994**, *6*, 181−195.
(4) Power, P. P. *Chem. Rev.* **2012**, *112*, 3482−3507.
(5) Alyea, E. C.; Bradley, D. C.; Copperthwaite, R. G. *J. Chem. Soc., Dalton Trans.* **1972**, 1580−1584.
(6) Bradley, D. C.; Copperthwaithe, R. G. *Inorg. Synth.* **1978**, *18*, 112−120.
(7) Bradley, D. C.; Copperthwaite, R. G. *J. Chem. Soc. D.* **1971**, 764−764.
(8) Ellison, J. J.; Power, P. P.; Shoner, S. C. *J. Am. Chem. Soc.* **1989**, *111*, 8044−8046.
(9) (a) Bradley, D. C.; Chisholm, M. H. *Acc. Chem. Res.* **1976**, *9*, 273−280. (b) Eller, P. G.; Bradley, D. C.; Hursthouse, M. B.; Meek, D. W. *Coord. Chem. Rev.* **1977**, *24*, 1−95. (c) Cummins, C. C. *Prog. Inorg. Chem.* **1998**, *47*, 885−936. (d) Alvarez, S. *Coord. Chem. Rev.* **1999**, *193*−*5*, 13−41.
(10) Fjeldberg, T.; Andersen, R. A. *J. Mol. Struct.* **1985**, *128*, 49−57.
(11) Bradley, D. C.; Hursthouse, M. B.; Rodesiler, P. F. *J. Chem. Soc. D.* **1969**, 14−15.
(12) Ghotra, J. S.; Hursthouse, M. B.; Welch, A. J. *J. Chem. Soc., Chem. Commun.* **1973**, 669−670.
(13) Köhn, R. D.; Kociok-Köhn, G.; Haufe, M. *Chem. Ber.* **1996**, *129*, 25−27.
(14) Putzer, M. A.; Magull, J.; Goesmann, H.; Neumüller, B.; Dehnicke, K. *Eur. J. Inorg. Chem.* **1996**, *129*, 1401−1405.
(15) Alyea, E. C.; Basi, J. S.; Bradley, D. C.; Chisholm, M. H. *Chem. Commun. (London).* **1968**, 495−495.

(16) Bradley, D. C.; Copperthwaite, R. G.; Cotton, S. A.; Sales, K. D.; Gibson, J. F. *J. Chem. Soc., Dalton Trans.* **1973**, 191−194.
(17) Alyea, E. C.; Bradley, D. C.; Copperthwaite, R. G.; Sales, K. D. *J. Chem. Soc., Dalton Trans.* **1973**, 185−191.
(18) Lappert, M. F.; Pedley, J. B.; Sharp, G. J.; Bradley, D. C. *J. Chem. Soc., Dalton Trans.* **1976**, 1737−1740.
(19) Bradley, D. C.; Fisher, K. J. *J. Am. Chem. Soc.* **1971**, *93*, 2058−2059.
(20) Olmstead, M. M.; Power, P. P.; Shoner, S. C. *Inorg. Chem.* **1991**, *30*, 2547−2551.
(21) Bradley, D. C.; Hursthouse, M. B.; Malik, K. M. A.; Möseler, R. *Transition Met. Chem.* **1978**, *3*, 253−254.
(22) Murray, B. D.; Power, P. P. *Inorg. Chem.* **1984**, *23*, 4584−4588.
(23) (a) Reiff, W. M.; LaPointe, A. M.; Witten, E. H. *J. Am. Chem. Soc.* **2004**, *126*, 10206−10207. (b) Reiff, W. M.; Schulz, C. E.; Whangbo, M.-H.; Seo, J. I.; Lee, Y. S.; Potratz, G. R.; Spicer, C. W.; Girolami, G. S. *J. Am. Chem. Soc.* **2009**, *131*, 404−405.
(24) (a) Zadrozny, J. M.; Atanasov, M.; Bryan, A. M.; Lin, C.-Y.; Rekken, B. D.; Power, P. P.; Neese, F.; Long, J. R. *Chem. Sci.* **2013**, *4*, 125−138. (b) Zadrozny, J. M.; Xiao, D. J.; Atanasov, M.; Long, G. J.; Grandjean, F.; Neese, F.; Long, J. R. *Nat. Chem.* **2013**, *5*, 577−581.
(25) Kahn, O. *Molecular Magnetism*; VCH−Wiley: New York, 1993; p 12.
(26) Caneschi, A.; Gatteschi, D.; Sessoli, R.; Barra, A. L.; Brunel, L. C.; Guillot, M. *J. Am. Chem. Soc.* **1991**, *113*, 5873−5874.
(27) Ishikawa, N.; Sugita, M.; Ishikawa, T.; Koshihara, S.; Kaizu, Y. *J. Am. Chem. Soc.* **2003**, *125*, 8694−8695.
(28) Bryan, A. M.; Merrill, W. A.; Reiff, W. M.; Fettinger, J. C.; Power, P. P. *Inorg. Chem.* **2012**, *51*, 3366−3373.
(29) Merrill, W. A.; Stich, T. A.; Brynda, M.; Yeagle, G. J.; Fettinger, J. C.; De Hont, R.; Reiff, W. M.; Schulz, C. E.; Britt, R. D.; Power, P. P. *J. Am. Chem. Soc.* **2009**, *131*, 12693−12702.
(30) Putzer, M. A.; Neumüller, B.; Dehnicke, K.; Magull, J. *Chem. Ber.* **1996**, *129*, 715−719.
(31) Pangborn, A. B.; Giardello, M. A.; Grubbs, R. H.; Rosen, R. K.; Timmens, F. J. *Organometallics* **1996**, *15*, 1518−1520.
(32) Panda, A.; Stender, M.; Olmstead, M. M.; Klavins, P.; Power, P. P. *Polyhedron* **2003**, *22*, 67−73.
(33) Wannagat, U.; Niederprum, H. *Chem. Ber.* **1961**, *94*, 1540−1547.
(34) Amonoo-Neizer, E. H.; Shaw, R. A.; Skovlin, D. O.; Smith, B. C. *Inorg. Synth.* **1966**, *8*, 19−22.
(35) Hope, H. *Prog. Inorg. Chem.* **1995**, *41*, 1−19.
(36) Sheldrick, G. M. *SADABS, Siemens Area Detector Absorption Correction*; Universität Göttingen: Göttingen, Germany, 2008.
(37) Sheldrick, G. M. *SHELXTL-2013 and SHELXL-2013*; Universität Göttingen: Göttingen, Germany, 1997.
(38) Dolomanov, O. V.; Bourhis, L. J.; Gildea, R. J.; Howard, J. A. K.; Puschmann, H. *Appl. Crystallogr.* **2009**, *42*, 339−341.
(39) Bain, G. A.; Berry, J. F. *J. Chem. Educ.* **2008**, *85*, 532−536.
(40) Horvath, B.; Möseler, R.; Horvath, E. G. *Z. Anorg. Allg. Chem.* **1979**, *450*, 165−171.
(41) Bradley, D. C.; Hursthouse, M. B.; Smallwood, R. J.; Welch, A. J. *J. Chem. Soc., Chem. Commun.* **1972**, 872−873.
(42) (a) Bartlett, R. A.; Power, P. P. *J. Am. Chem. Soc.* **1987**, *109*, 7563−7564. (b) Chen, H.; Bartlett, R. A.; Dias, H. V. R.; Olmstead, M. M.; Power, P. P. *J. Am. Chem. Soc.* **1989**, *111*, 4338−4345.
(43) Shannon, R. D. *Acta Crystallogr., Sect. A: Cryst. Phys., Diffr., Theor. Gen. Crystallogr.* **1976**, *A32*, 751−768.
(44) Layfield, R. A.; McDouall, J. J. W.; Scheer, M.; Schwarzmaier, C.; Tuna, F. *Chem. Commun.* **2011**, *47*, 10623−10625.
(45) Ingleson, M. J.; Layfield, R. A. *Chem. Commun.* **2012**, *48*, 3579−3589.
(46) Lin, P. -H.; Smythe, N. C.; Gorelsky, S. I.; Maguire, S.; Henson, N. J.; Korobkov, I.; Scott, B. L.; Gordon, J. C.; Baker, R. T.; Murugesu, M. *J. Am. Chem. Soc.* **2011**, *133*, 15806−15809.
(47) Andres, H.; Bominaar, E. L.; Smith, J. M.; Eckert, N. A.; Holland, P. L.; Münck, E. *J. Am. Chem. Soc.* **2002**, *124*, 3012−3025.
(48) Panda, A.; Stender, M.; Wright, R. J.; Olmstead, M. M.; Klavins, P.; Power, P. P. *Inorg. Chem.* **2002**, *41*, 3909−3916.
(49) (a) Chen, H.; Bartlett, R. A.; Olmstead, M.; Power, P. P.; Shoner, S. C. *J. Am. Chem. Soc.* **1990**, *112*, 1048−1055. (b) Ni, C.; Fettinger, J. C.; Long, G. J.; Power, P. P. *Inorg. Chem.* **2009**, *48*, 2443−2448. (c) Ni, C.; Stich, T. A.; Long, G. J.; Power, P. P. *Chem. Commun.* **2010**, 4466−4468.
(50) Hope, H.; Olmstead, M. M.; Murray, B. D.; Power, P. P. *J. Am. Chem. Soc.* **1985**, *107*, 712−713.
(51) Zadrozny, J. M.; Long, J. R. *J. Am. Chem. Soc.* **2011**, *133*, 20732−20734.
(52) Chilton, N. F.; Anderson, R. P.; Turner, L. D.; Soncini, A.; Murray, K. S. J. *Comput. Chem.* **2013**, *34*, 1164−1175.
(53) Gomez-Coca, S.; Cremades, E.; Aliaga-Alcade, N.; Ruiz, E. *J. Am. Chem. Soc.* **2013**, *135*, 7010−7018.
(54) Ruamps, R.; Batchelor, L.; Maurice, R.; Gogoi, N.; Jiménez-Lozano, P.; Guihéry, N.; de Graaf, C.; Barra, A.-L.; Sutter, J.-P.; Mallah, T. *Chem.—Eur. J.* **2013**, *19*, 950−956.
(55) Campanion, A. L.; Komarynsky, M. A. *J. Chem. Educ.* **1964**, *41*, 257−262.
(56) Neese, F.; Pantazis, D. A. *Faraday Discuss.* **2011**, *148*, 229−238.
(57) The mischaracterization of "Co{N(SiMe$_3$)$_2$}$_2$" as its THF adduct **4** is partly understandable on the basis of its very high air sensitivity, and the fact that no elemental analysis was obtained because of this characteristic.[1a] Furthermore, the isolation and characterization of stable THF-metal complexes was not common at the time the original report was published. In addition, the recording and processing of X-ray crystallographic data were difficult and time-consuming tasks in the early 1960s. There is irony in the fact that, since "Co{N(SiMe$_3$)$_2$}$_2$" was first reported,[1a] the THF-free complex **1** has been synthesized numerous times and its structure determined in the vapor phase by ged,[2] and in the solid state by X-ray crystallography.[22]

NOTE ADDED AFTER ASAP PUBLICATION

This paper was published on the Web on October 10, 2013, with minor text errors throughout the paper. The corrected version was reposted on October 21, 2013.